



Sustainable Synthesis of Copper Oxide Nanoparticles Using *Aquilaria Malaccensis* (Agarwood) Leaf Extract as Reducing Agent

Sathia Lingam Valan¹, Alice Escalante De Cruz^{1*}, Patricia Jayshree Jacob¹,
Sinouvassane Djearamane²

¹School of Applied Sciences, Faculty of Engineering, Science and Technology, Nilai University, Persiaran
Universiti, Putra Nilai 1, Persiaran Kolej Bbn, 71800 Nilai, Negeri Sembilan, Malaysia

²Department of Biomedical Science, Faculty of Science, Universiti Tunku Abdul Rahman, Kampar, 31900,
Perak, Malaysia

Abstract. This paper reports the green synthesis of Copper Oxide nanoparticles (CuO NPs) using *Aquilaria malaccensis* (agarwood) leaf extract. The main objective of this study was to evaluate the potential of using *A. malaccensis* leaf extract as a biogenic medium to generate CuO NPs with antimicrobial potential. The procedure employed was to add 5 mM copper sulfate ($\text{CuSO}_4 \cdot 5\text{H}_2\text{O}$) as the precursor to *A. malaccensis* leaf extract to study the generation of CuO NPs under different incubation conditions such as methods of crude extract preparation, precursor concentration and incubation temperature. The results demonstrated that the boiled leaf extract reacted with 5 mM $\text{CuSO}_4 \cdot 5\text{H}_2\text{O}$ at pH 6 and incubated under non-shaking conditions at 70 °C, resulting in a high rate of CuO NPs formation and depicting a UV absorbance peak of 430 nm. Green synthesized CuO NPs were characterized using field emission scanning electron microscopy (FESEM) and energy-dispersive X-ray spectroscopy (EDX), Fourier-transform infrared spectroscopy (FTIR), X-ray diffraction (XRD), and transmission electron microscopy (TEM). FESEM and TEM revealed that the nanoparticles are mainly spherical, ranging from 6 to 32 nm. Antimicrobial studies showed that 20 μL and 40 μL of 70 $\mu\text{g}/\mu\text{L}$ CuO NPs displayed potent inhibition towards Gram-positive bacteria *Bacillus subtilis*, with the average zone of inhibition measuring 24.43 ± 0.10 mm and 27.31 ± 0.13 mm, respectively.

Keywords: Antimicrobial; *Aquilaria malaccensis*; Copper oxide nanoparticles; Green synthesis; Phytochemical

1. Introduction

Copper is a prominent metal with a wide range of applications due to its pertinent properties such as electrical, conductivity, optical, catalytic, and antimicrobial applications compared to other metallic structures. At the nano-size, copper has been used extensively as gas sensors, catalysts, and superconductors, in photovoltaic devices such as solar panels, dye removal from wastewater, and agricultural sectors (Jiang et al., 2015; Sundar et al., 2018; Sone et al., 2020).

Moreover, copper oxide nanoparticles (CuO NPs) have excellent antifungal and antimicrobial potential, thus emerging as a promising tool for many industries, including

*Corresponding author's email: alice_cruz@nilai.edu.my, Tel.: +60-6-8502338; Fax: +60-6-7998502
doi: [10.14716/ijtech.v13i5.5845](https://doi.org/10.14716/ijtech.v13i5.5845)

food, medical and pharmaceutical, and agriculture (Sivaraj et al., 2014; Chalandar et al., 2017; Maqbool et al., 2017).

The standard routes to generate CuO NPs entail methods delineated using physical or chemical processes such as hydrothermal, sol-gel, and solid-state reactions (Sohrabnezhad & Valipour, 2013; Quirino et al., 2018; Dorner et al., 2019; Muktaridha et al., 2021). Although these processes can be modulated to produce well-defined nanoparticles of preferred morphology and size, the toxic solvents and the byproducts threaten the environment. Additionally, some of these methods incur a high cost of investment due to their high energy requirements, such as the vapor transport method, which works well in high temperatures up to 1,400°C (Sabir et al., 2014), and the necessity to use specialized equipment such as ball grinding (Yadav & Vasu, 2016). On the other hand, green synthesis, or the use of biomaterials as a reducing agent in the generation of nanostructures, has emerged as a method of choice since it is facile, cost-effective, and environmentally safe (Kayalvizhi et al., 2020; Siddiqi and Husen, 2020). Processes using green synthesis do not pose high energy requirements or the usage of specialized equipment (Sankar et al., 2014; Rajesh et al., 2018), leading to a significant reduction in cost. They are also efficient and have less reaction time (Omar et al., 2020). Work on such processes using plant extracts needs to be intensified to scale it up for industrial production. Extracts from plant structures such as leaves, seeds, bark, flowers, and stem contain phytochemicals that can be used as the bioreducing or capping agent in generating metallic nanoparticles from their aqueous form. Several plant extracts such as *Carica papaya* (Sankar et al., 2014), *Syzygium aromaticum* flower bud (Rajesh et al., 2018), and *Azadirachta indica* leaf (Nagar and Devra, 2018) have been explored as natural reducing and capping agents for the synthesis of copper nanoparticles. In contrast, the leaf of *Aloe vera* (Kumar et al., 2015) and *Annona muricata* (Kayalvizhi et al., 2020) have been explored to synthesize CuO NPs. In this study, *Aquilaria malaccensis* was introduced as an alternative reducing/capping agent for the synthesis of CuO NPs. Din et al. (2017) observed that a reactive hydrogen atom in plant flavonoids reduces Cu^{2+} to form copper nuclei in the nucleation of CuO NPs. Therefore, it is assumed that flavonoids in plant extracts act as reducing agents and play an essential role in the nucleation of CuO NPs (Ferrando, 2016). Capping agents act as binding molecules which modulate the surface chemistry of the nanoparticles and shield them to prevent the over-growth of the nanoparticles, which causes agglomeration (Javed et al., 2020).

Aquilaria malaccensis is rich in phytochemicals such as flavonoids, alkaloids, squalene, saponins, steroids, terpenoids, tannins, n-hexadecanoic acid, tetramethyl-2-hexadecane-1-ol, octadecatrienoic acid and phenols, which has the potential to be utilized as reducing and capping agents in the synthesis of metal nanoparticles (Khalil et al., 2013; Buniyamin et al., 2021). The presence of different phytochemicals is important because flavonoids can undergo a tautomeric transformation and release reactive hydrogen atoms. This mechanism was discovered while reducing metal ions into metal nanoparticles (Singh et al., 2017). Whereas phenolic compound has hydroxyl and ketone groups which help to bind and chelate metal (Singh et al., 2017). In addition, glucose, fructose, and amino acids can reduce metal ions differently (Panigrahi et al., 2004). Hence, the richness of phytochemicals in the plant extract is essential in synthesizing nanoparticles. A previous study has shown that leaf extract of *A. malaccensis* has been explored in synthesizing tin oxide nanoparticles via the reduction process (Buniyamin et al., 2021). The study's novelty is that *A. malaccensis* leaf extract was used to explore the synthesis of CuO NPs without using expensive techniques or toxic chemicals. Therefore, the objective of this study was to study the potential of *A. malaccensis* leaf extract as a reducing agent in the fabrication of CuO NPs and to characterize these nanostructures using standard techniques such as UV-Visible

spectrophotometry, FTIR, XRD, EDX, FESEM, and TEM. The capability of CuO NPs to inhibit bacterial growth was also investigated.

2. Methods

2.1. Collection of Plant Samples and Extract Preparation

1000 g of *A. malaccensis* leaves were collected in the garden of Nilai University, Negeri Sembilan, Malaysia (2°48'59.2"N 101°46'05.2"E). The leaves were washed with tap water and then distilled water to remove tiny dust particles and dehydrated in the oven at 60 °C for two days. The dried leaves were crushed into a fine powder using a mechanical blender (Xinganbangle, China) and refrigerated at 4 °C. Leaf extract was prepared by adding 2 g of powdered leaf samples into 100 ml of distilled water and boiling for 10 minutes. This mixture was cooled to room temperature and then centrifuged (UNIVERSAL 16R, Model LWB-122D) at 4000 rpm for 10 minutes to separate the particulate and the extract. The supernatant was transferred to a new tube and centrifuged for 20 minutes. The purified supernatant was stored in the refrigerator at 4 °C to synthesize CuO NPs.

2.2. The Influence of Process Parameters on the Green Synthesis of CuO NPs

CuO NPs were synthesized by mixing an equal volume of aqueous leaf extract with 5 mM aqueous CuSO₄·5H₂O (Bendosen, Malaysia) as a precursor. A color change from light brown to dark brown/reddish brown indicated the formation of CuO NPs. The reaction mixture was centrifuged at 15,000 rpm for 20 minutes, and the pellet was washed three times using distilled water. The pellet was then crushed after drying in the oven at 60 °C for 2 h. Powdered CuO NPs were calcinated (Lindberg/Blue M, United States) at 600 °C for 3 h. The influence of various process parameters on the synthesis of CuO NPs was observed at different concentrations (5 mM and 10 mM) of the precursor, CuSO₄·5H₂O, extract preparation through boiling for 10 minutes or heating at 70 °C for 20 minutes, agitation of the reaction mixture and pH (pH 6, 9 and 12) of the reaction mixture. The schematic illustration of the green synthesis of CuO NPs is depicted in Figure 1.

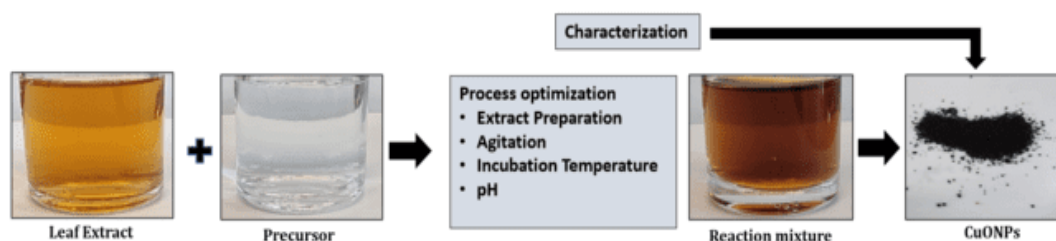


Figure 1 Schematic illustration of green synthesis of CuO NPs

2.3. Characterization of Green Synthesized CuO NPs

The optical properties of CuO NPs were characterized using a UV-visible absorption spectrophotometer (HALO RB-10 Dynamica, Australia). Fourier transform infrared spectroscopy (FTIR)(Perkin Elmer, Spectrum 400, United States), X-ray diffraction (XRD) (D8 Advance, Bruker AXS, Germany), Field emission scanning microscopy (FESEM)(ZEISS, SUPRA 55VP, Germany) with energy-dispersive X-ray spectroscopy (EDX)(AZtecEnergy EDX 80 mm X-Max SDD detector, United Kingdom), and transmission electron microscopy (TEM)(Talos L120C, ThermoFisher, United States) to verify the generation of CuO NPs and to assess its morphology, size, and elemental composition.

2.4. Antimicrobial Activity of CuO NPs

The agar well diffusion method evaluated antimicrobial activity against Gram-positive (*Bacillus subtilis*—ATCC 6051) bacteria. Nutrient agar plates were inoculated using a cotton

swab dipped in 10^6 CFU McFarland Standard bacterial suspensions. Wells of 6 mm diameter were bored in the inoculated plates using a sterile borer. These wells were then loaded with 40 μ l green synthesized and commercial CuO NPs (Copper (II) oxide, 30-50 nm, Alfa Aesar) (70 μ g/ml). Control wells were filled with 40 μ L of *A. malaccensis* leaf extract and ampicillin (Santa Cruz, California) (70 μ g/ μ l) as the positive control. These plates were incubated at 37 °C for 24 h, and antibacterial activities were evaluated by measuring the inhibition zone diameter around the wells.

3. Results and Discussion

3.1. Optimization of Different Parameters in Biosynthesizing CuO NPs

3.1.1. Preparation of Crude Leaf Extract of *A. Malaccensis*

Leaf extract preparation under different conditions was explored in this section. First, adding 5 mM $\text{CuSO}_4 \cdot 5\text{H}_2\text{O}$ to leaf extract, which was boiled for 10 minutes, showed intense color change compared to heating the leaf extract at 70 °C for 20 minutes. The leaf samples used in this study were powdered to increase the surface contact between the sample and the solvent. Although the surface contact of the leaf powder sample was achieved by crushing yet, boiling the leaf extract at 100 °C for 10 minutes is assumed to aid in the rapid release of phytochemicals, causing the increase in color intensity of the reaction mixture compared to heating at 70 °C for 20 minutes. UV-Vis analysis showed a uniform size distribution of the synthesized CuO NPs using boiled leaf extract than the heating preparation. However, both leaf extracts validate the peak at 420 nm.

3.1.2. Agitation of the Reaction Mixture

Agitation of the reaction mixture is demonstrated to influence the green synthesis of CuO NPs using *A. malaccensis* aqueous leaf extract. The intensity of color change in the reaction mixture increased in the reaction mixture, which was left without agitation compared to agitating the reaction mixture. An increase in the intensity of the brown pigmentation in the reaction mixture correlates to the rise in the formation of CuO NPs, stipulating that non-agitation conditions were more conducive for the green synthesis of CuO NPs. The reaction mixture without agitation demonstrated a higher absorbance intensity than the agitated reaction, suggesting a higher rate of CuONP formation.

3.1.3. Concentration of the Precursor

CuO NPs formation depended on the concentration of the precursor, aqueous $\text{CuSO}_4 \cdot 5\text{H}_2\text{O}$, used for the reaction mixture. The reaction mixture was observed at 5 mM and 10 mM $\text{CuSO}_4 \cdot 5\text{H}_2\text{O}$. The resulting reaction mixture showed that when 10 mM precursor was used, CuO NPs aggregated by the first 20 minutes of reaction. Aggregation of nanoparticles results in bulk form and may show different diameters and particle size distribution (Dang et al., 2011a). According to Dang et al. (2011b), the copper particles aggregate during nuclei formation to reduce the total surface energy. This aggregation may result from attractive Van Der Waals forces between the crystals formed. Also, another reported article stated that an increase in precursor from 6 mM to 7.5 mM concentration led to increasing particle size, which significantly resulted in aggregation and growth of particle size (Nagar and Devra, 2018). On the other hand, a study from Kumar et al. (2015) proves that copper nitrate at a concentration of 10 mM reacts with leaf extract of *Aloe vera* leaf extract, resulting in overlapping and aggregation of smaller particles. Hence, copper sulfate precursor at 10 mM became very hard to characterize using UV-Vis spectrophotometer due to the growth of precipitates; however, the precursor concentration of 5 mM was stable without any precipitation observed for up to 3 weeks.

3.1.4. Incubation Temperature of the Reaction Mixture

The incubation temperature of the reaction mixture is known to influence the formation of metallic nanoparticles in green synthesis. Nagar and Devra (2018) showed that the conversion rate of Cu^{2+} to CuO NPs gradually increased as the temperature rose from 60 to 85 °C due to a rapid nucleation rate. The UV-Vis spectrophotometer results recorded showed that the formation rate of CuO NPs doubled at 70 °C compared to room temperature, confirming the postulation that an increase in reaction temperature increases the reaction rate reducing Cu^{2+} metal ions to form the nuclei of the CuO NPs (Joshi et al., 2019).

3.1.5. The pH of the Reaction Mixture

Green synthesis of CuO NPs using aqueous extract of *A. malaccensis* leaf extract was examined over a broad pH range (9 and 12). As reflected in the absorbance, changes in pH highly affected the surface plasmon resonance (SPR) of the CuO NPs. It was observed that the absorbance peak shifted from 430 nm at pH 6 to 340 nm in alkaline pH of pH9 and pH12, confirming the observation made by Thamer et al. (2018). According to Nagar and Devra (2018), pH is essential in the synthesis of nanoparticles, and changes in pH directly affect the rate of synthesis and the morphology of nanoparticles. A change in pH affects the charges of biomolecules, affecting their stabilizing and capping ability. It was discovered that nanoparticles were not formed in acidic conditions such as pH 4.7 due to the suppressing effect of acidic pH that inactivated biomolecules. Raising the pH to pH 6 and pH 6.6 resulted in the synthesis of more small-sized nanoparticles due to the availability of functional groups in biomolecules responsible for copper binding. Even higher pH was discovered to be efficient in the synthesis of nanoparticles; however, nanoparticles tend to form large size nanoparticles due to agglomeration. Hulkoti and Taranath (2014) observed that the pH of the reaction mixture influences the size, shape, and composition of CuO NPs.

Overall, it can be found that using a crude extract prepared by boiling for 10 minutes using 5 mM $\text{CuSO}_4 \cdot 5\text{H}_2\text{O}$ at pH 6 and incubated under the non-shaking condition at an incubation temperature of 70 °C results in a rapid and increased formation of CuO NPs. Further analysis was carried out to characterize the synthesized CuO NPs using FESEM, EDX, FTIR, XRD, and TEM to determine the size distribution, shape, and composition of the CuO NPs.

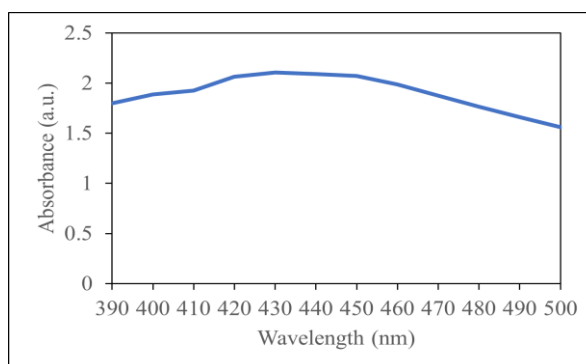


Figure 2 UV-Vis absorption spectra of green synthesized CuO NPs

3.2. Characterization of CuO NPs

3.2.1. UV Spectroscopy

The addition of the *A. malaccensis* aqueous leaf extract to the precursor, aqueous $\text{CuSO}_4 \cdot 5\text{H}_2\text{O}$, resulted in a color change from light brown to dark brown in the reaction mixture after 2 h, which intensified after 24 h. The indication of the formation of CuO NPs in the reaction mixture was confirmed through an SPR peak observed at a wavelength of

430 nm (Figure 2) using UV spectrophotometry after 24 h incubation based on the reports of Thamer et al. (2018) and Naika et al. (2015), which reported SPR peaks located at wavelengths of 392 nm and 415 nm, respectively as indicative of the formation of CuO NPs.

3.2.2. Field Emission Scanning Electron Microscopy and Dispersive X-ray Spectrograph

The result obtained from FESEM is depicted in Figure 3a, clearly showing the presence of CuO NPs that demonstrated a degree of aggregation. This feature was characteristic of green synthesized metallic nanoparticles. Mali et al. (2019) reported that the aggregation of CuO NPs could be attributed to the high viscosity of *E. axillare* leaf extract. The size of the CuO NPs depicted in the FESEM micrograph taken at a 150,000X magnification in Figure 3a ranged between 22.3, 24.6, and 32.0 nm, indicating well-defined nanoparticles. A simple particle size analysis using Image J and OriginPro 2021 is represented in the histogram in Figure 3b, where the average particle size obtained was 19 nm. To confirm the formation of CuO NPs, EDX analysis was performed. Different areas were focused during the EDX measurement, and the corresponding peaks are shown in Figure 3c. Both copper (Cu) and oxygen (O) are evident in the biosynthesized nanoparticles in the EDX spectrum. The weight composition of Cu and O were 55.5% and 21.0%, respectively, whereas the atomic percentage was 21.86% and 32.88%. The presence of a small amount of carbon (C), phosphorus (P), and sulphur (S) could be due to the presence of organic compounds in the crude leaf extract during synthesis (Rajesh et al., 2018; Mali et al., 2019).

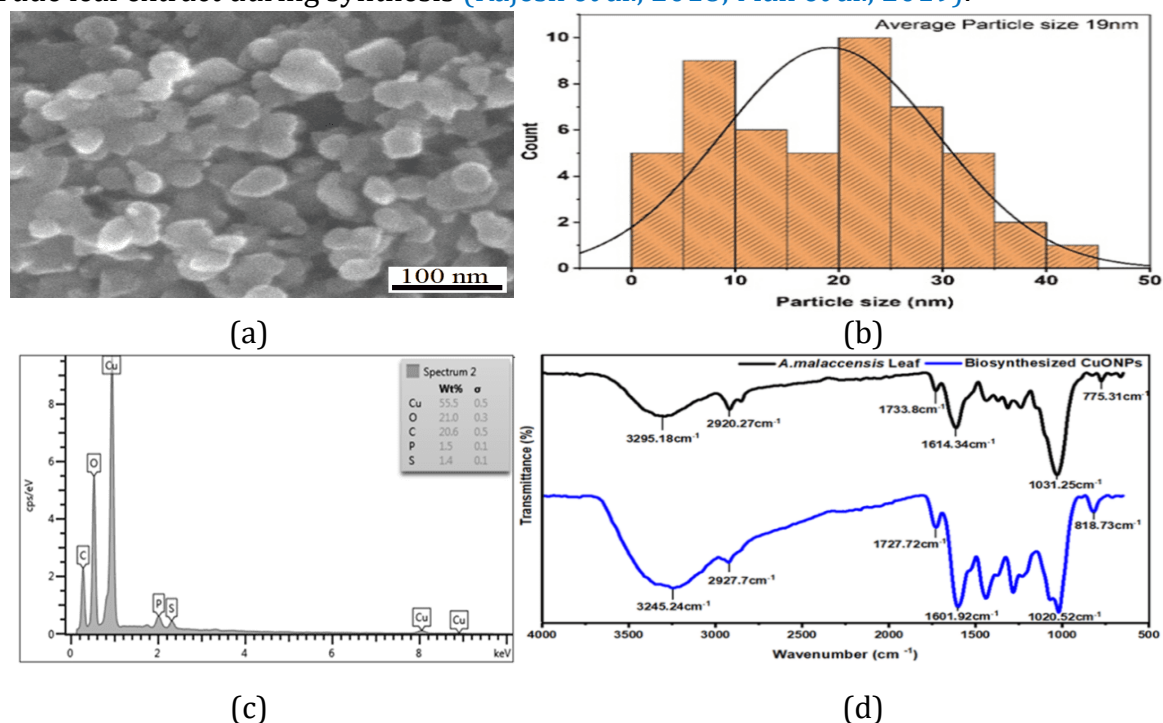


Figure 3 (a) FESEM image, (b) Histogram of the particle size distribution based on FESEM image, (c) EDX spectrum, and (d) FTIR of biosynthesized CuO NPs

3.2.3. FTIR Analysis

FTIR spectroscopy was used to analyze the functional group of active components present in the sample based on the peak values. The result of FTIR analysis on the powdered leaf sample of *A. malaccensis* and synthesized CuO NPs is shown in Figure 3d. The broad vibrational peak at 3295.18 cm^{-1} is due to the O-H stretching vibration (Helmiyati and Anggraini, 2019) of surface hydroxyl groups, indicating adsorbed water molecules. This phenomenon arises due to nanocrystals' high surface-to-volume ratio, which absorbs high moisture (Sundar et al., 2018). The small band found at 2920.37 cm^{-1} corresponds to

methylene's C-H asymmetrical/ symmetrical stretch. The peak in 1733.8 cm^{-1} relates to the carbonyl group (C=O) ester. The peak at 1614.34 cm^{-1} corresponds to a secondary amine group (N-H) stretching. The small band in 1439.2 cm^{-1} reveals the carbonate ion, whereas the peak at 1315.93 cm^{-1} represents aromatic primary amine C-N stretch, which is aromatic amino acids. A sharp peak at 1031.25 cm^{-1} reveals the presence of methylene (CH_2). The FTIR spectrum (Figure 3d) of CuO NPs demonstrates that the $3295.18, 2920.37, 1733.8, 1614.34, 1439.2,$ and 1315.93 cm^{-1} peaks were shifted to new position of $3245.24, 2927.7, 1727.72, 1439.65, 1282.83,$ and 1020.52 cm^{-1} respectively in the region of $650\text{-}4000\text{ cm}^{-1}$. The previous study by [Osuntokun et al. \(2017\)](#) reported that a single metal atom bonded to more than one oxygen atom commonly has an absorbance value of $1020\text{-}970\text{ cm}^{-1}$. This observation applies to several metal oxides. In this case, the sharp peak at 1020.52 cm^{-1} is assumed to correspond to CuO NPs. The phytochemical compound in *A. malaccensis* leaf extracts further functions as a reducing agent for synthesizing CuO NPs, confirmed by the FTIR result.

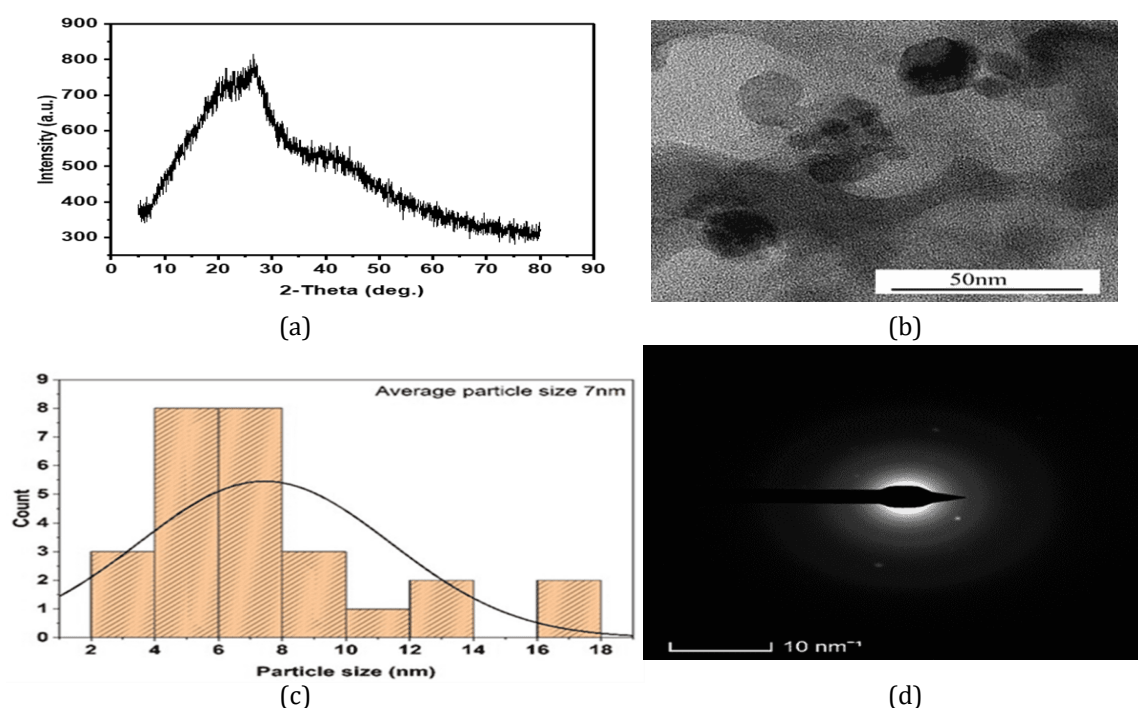


Figure 4 (a) XRD pattern of biosynthesized CuO NPs (b) TEM image of CuO NPs, (c) Histogram of the particle size distribution based on TEM image, and (d) Intermittent dots on SAED

3.2.4. X-ray Diffraction Analysis

XRD analysis exposed the crystalline nature of the CuO NPs, as shown in Figure 4a. XRD micrograph showed small distinct diffraction peaks at $21.74, 32.95,$ and 42.14 . These corresponding peaks represent (100), (110), and (200) of CuO NPs primitive structure. The grain size of CuO NPs formed in the bio-reduction process was measured using the Debye-Scherrer formula ($D = k\lambda/\beta \cos \theta$), where D is the average crystalline size, k represents constant 1, λ is the wavelength of x-ray source (0.15406 nm), β is the angular line full width at half maximum (FWHM) intensity in radians and θ the Bragg's angle. The XRD pattern showed that the average crystallite size was 1.08 nm .

3.2.5. Transmission Electron Microscopy

TEM analysis further confirmed the crystalline nature of the green synthesized CuO NPs, found as clusters due to aggregation, as shown in Figure 4b. The CuO NPs did not show

a uniform distribution and ranged from 6nm to 22 nm (Figure 4b) in size. Particle size analysis from the TEM micrograph was done using ImageJ and OriginPro 2021 and shown in a histogram (Figure 4c), where the average particle size obtained was 7 nm. Intermittent dots on Selected Area Electron Diffraction (SAED) on the concentric circle confirmed the crystalline nature of green synthesized CuO NPs, as depicted in Figure 4d. Similar results were reported by [Mali et al. \(2019\)](#) and [Nabila and Kannabiran \(2018\)](#). On a microscopic scale, the nanoparticles showed good dispersion in bio-reduced aqueous solution, which is explained through the results of the SAED.

3.2.6. Antibacterial Activity of the CuO NPs

Table 1 shows the mean diameter of inhibition zones (in mm) for three replicates containing CuO NPs suspension. The negative control used were *A. malaccensis* leaf extract, CuSO₄.5H₂O, and commercial CuO NPs. *A. malaccensis* leaf extract showed no inhibition effect due to no formation of clear inhibited zones on bacteria *B. subtilis*. However, 100mM CuSO₄.5H₂O showed an inhibition effect (26.03 ± 0.19 mm). Increasing the concentration of CuSO₄.5H₂O to 200 mM resulted in an increased diameter of the inhibition zones, 31.83 ± 0.29 mm. Copper has been utilized as an alternative antibacterial agent due to its novel and promising effect on nosocomial infections ([Benhalima et al., 2019](#)). Copper can also produce reactive oxygen species (ROS), inactivate enzymes, modify cell walls, and alter nucleic acid synthesis, significantly inhibiting nosocomial infections' growth ([Gant et al., 2007](#)). Hence, the presence of the Cu element in CuSO₄. 5H₂O inhibits the growth of bacteria such as *B. subtilis* (gram-positive) in the present study. Increasing the treatment concentration will also increase the availability of copper ions to induce ROS and other activity towards the bacteria; therefore, the inhibition effect on the bacteria such as *B. subtilis* was increased as the concentration was also increased. On the other hand, 20 µL of commercial CuO NPs can inhibit *B. subtilis* (26.60 ± 0.47 mm). A similar observation was found using biosynthesized CuO NPs where an inhibition zone of 24.43 ± 0.10 mm and 27.31 ± 0.13 mm, respectively, were obtained when 20 µL and 40 µL of biosynthesized CuO NPs on *B. subtilis*. These results may indicate that the CuO NPs synthesized using *A. malaccensis* leaf extract are less toxic than commercial CuO NPs presumably produced by chemical methods. The reduced toxicity could be due to the smaller size of CuO NPs generated through green processes (size: 6 - 32nm) compared to chemically synthesized ones (30 to 50nm), as explained by [Letchumanan et al. \(2021\)](#).

Table 1 Antibacterial activity of biosynthesized CuO NPs using the well diffusion method

Treatment	Inhibition (mm) ± SE.
Leaf Extract (20 µL)	0 ^a
CuSO ₄ .5H ₂ O (100mM)	26.03 ± 0.19 ^b
CuSO ₄ .5H ₂ O (200mM)	31.83 ± 0.29 ^c
Commercial CuO NPs (70 µg / µL, 20 µL)	26.60 ± 0.47 ^{bd}
Commercial CuO NPs (70 µg / µL, 40 µL)	29.98 ± 0.24 ^e
Biosynthesized CuO NPs (70 µg / µL, 20 µL)	24.43 ± 0.10 ^f
Biosynthesized CuO NPs (70 µg / µL, 40 µL)	27.31 ± 0.13 ^{dg}
Ampicillin (70 µg / µL, 20 µL)	40.28 ± 0.16 ^h

4. Conclusions

A facile, cost-effective, and sustainable synthesis of CuO NPs was achieved using the leaf extract of *A. malaccensis* as a reducing agent. Studies on reaction conditions showed that leaf extract prepared by boiling for 10 minutes and incubated under the non-shaking condition with the precursor at 70 °C and pH 6 resulted in rapid and increased formation of CuO NPs. The UV-Visible spectrophotometry analysis revealed the SPR peak at 430 nm.

FTIR result confirms the phytochemicals from *A. malaccensis* leaf extract responsible for the synthesis of CuO NPs. XRD spectra confirmed the crystalline nature of CuO NPs with an average crystallite size of 1.08 nm. FESEM, TEM, and EDX revealed the presence of spherical CuO NPs with an average particle size of 6 to 32 nm. This method proves that CuO NPs can be synthesized without toxic solvents or high-cost equipment. Antimicrobial studies showed that these CuO NPs at the concentration of 20 and 40 μL of 70 $\mu\text{g}/\mu\text{L}$ could inhibit the growth of Gram-positive *B. subtilis* with an average inhibition zone of 24.43 ± 0.10 mm and 27.31 ± 0.13 mm. Further studies should be conducted to determine the antimicrobial potential of these nanoparticles in a broader range of microbial pathogens.

Acknowledgements

The authors would like to thank Chris Izaak Jones and Cornelius Berani Anak Paul Ringo for their assistance in the experiments and Nilai University for providing the necessary facilities. This study was supported by the Research and Innovation of Private Higher Education Network (RIPHEN) in the Digital Futures project (MMUE/200003) framework coordinated by Koo Ah-Choo, Multimedia University, Malaysia, and the Malaysian Institute of Retirement Management (MIRM).

References

- Benhalima, L., Amri, S., Bensouilah, M., Ouzrout, R., 2019. Antibacterial Effect of Copper Sulfate Against Multi-Drug Resistant Nosocomial Pathogens Isolated from Clinical Samples. *Pakistan Journal of Medical Sciences*, Volume 35(5), pp. 1322–1328
- Buniyamin, I., Akhir, R.M., Asli, N.A., Khusaimi, Z., Mahmood, M.R., 2021. Biosynthesis of SnO₂ Nanoparticles by Aqueous Leaves Extract of *Aquilaria Malaccensis* (agarwood). *In: IOP Conference Series: Materials Science and Engineering*, Volume 1092(1), p. 012070
- Chalandar, H.E., Ghorbani, H.R., Attar, H., Alavi, S.A., 2017. Antifungal Effect of Copper and Copper Oxide Nanoparticles Against *Penicillium* on Orange Fruit. *Biosciences Biotechnology Research Asia*, Volume 14(1), pp. 279–284
- Dang, T.M.D., Le, T.T.T., Fribourg-Blanc, E., Dang, M.C., 2011a. The Influence of Solvents and Surfactants on the Preparation of Copper Nanoparticles by a Chemical Reduction Method. *Advances in Natural Sciences: Nanoscience and Nanotechnology*, Volume 2(2), p. 025004
- Dang, T.M.D., Le, T.T.T., Fribourg-Blanc, E., Dang, M.C., 2011b. Synthesis and Optical Properties of Copper Nanoparticles Prepared by a Chemical Reduction Method. *Advances in Natural Sciences: Nanoscience and Nanotechnology*, Volume 2(1), p. 015009
- Din, M.I., Arshad, F., Hussain, Z., Mukhtar, M., 2017. Green Adeptness in the Synthesis and Stabilization of Copper Nanoparticles: Catalytic, Antibacterial, Cytotoxicity, and Antioxidant Activities. *Nanoscale Research Letters*, Volume 12(1), pp. 1–15
- Dörner, L., Cancellieri, C., Rheingans, B., Walter, M., Kägi, R., Schmutz, P., Kovalenko, M.V., Jeurgens, L.P., 2019. Cost-effective Sol-gel Synthesis of Porous CuO Nanoparticle Aggregates with Tunable Specific Surface Area. *Scientific Reports*, Volume 9(1), pp. 1–13
- Ferrando, R., 2016. Chapter 3-Synthesis and Experimental Characterization of Nanoalloy Structures. *Structure and Properties of Nanoalloys*, Volume 10, pp. 47–74.
- Gant, V.A., Wren, M.W., Rollins, M.S., Jeanes, A., Hickok, S.S., Hall, T.J., 2007. Three Novel Highly Charged Copper-based Biocides: Safety and Efficacy Against Healthcare-

- Associated Organisms. *Journal of Antimicrobial Chemotherapy*, Volume 60(2), pp. 294–299
- Helmiyati, Anggraini, Y., 2019. Nanocomposites Comprising Cellulose and Nanomagnetite as Heterogeneous Catalysts for the Synthesis of Biodiesel from Oleic Acid. *International Journal of Technology*, Volume 10(4), pp. 798–807
- Hulkoti, N.I., Taranath, T.C., 2014. Biosynthesis of Nanoparticles Using Microbes: A Review. *Colloids and Surfaces B: Biointerfaces*, Volume 121, pp. 474–483
- Javed, R., Zia, M., Naz, S., Aisida, S.O., Ao, Q., 2020. Role of Capping Agents in the Application of Nanoparticles in Biomedicine and Environmental Remediation: Recent Trends and Future Prospects. *Journal of Nanobiotechnology*, Volume 18(1), pp. 1–15
- Jiang, T., Wang, Y., Meng, D., Yu, M., 2015. Facile Synthesis and Photocatalytic Performance of Self-assembly CuO Microspheres. *Superlattices and Microstructures*, Volume 85, pp. 1–6
- Joshi, A., Sharma, A., Bachheti, R.K., Husen, A., Mishra, V.K., 2019. Plant-mediated Synthesis of Copper Oxide Nanoparticles and Their Biological Applications. *Nanomaterials and Plant Potential*, Volume 2019, pp. 221–237
- Kayalvizhi, S., Sengottaiyan, A., Selvankumar, T., Senthilkumar, B., Sudhakar, C., Selvam, K., 2020. Eco-friendly Cost-effective Approach for Synthesis of Copper Oxide Nanoparticles for Enhanced Photocatalytic Performance. *Optik*, Volume 202, p. 163507
- Khalil, A.S., Rahim, A.A., Taha, K.K., Abdallah, K.B., 2013. Characterization of Methanolic Extracts of Agarwood Leaves. *Journal of Applied and Industrial Sciences*, Volume 1(3), pp. 78–88
- Kumar, P.P.N., Shameem, U., Kollu, P., Kalyani, R.L., Pammi, S.V.N., 2015. Green Synthesis of Copper Oxide Nanoparticles Using *Aloe Vera* Leaf Extract and its Antibacterial Activity Against Fish Bacterial Pathogens. *BioNanoScience*, Volume 5(3), pp. 135–139
- Letchumanan, D., Sok, S.P., Ibrahim, S., Nagoor, N.H., Arshad, N.M., 2021. Plant-based Biosynthesis of Copper/Copper Oxide Nanoparticles: An Update on Their Applications in Biomedicine, Mechanisms, and Toxicity. *Biomolecules*, Volume 11(4), pp. 1–27
- Mali, S.C., Raj, S., Trivedi, R., 2019. Biosynthesis of Copper Oxide Nanoparticles Using *Encostemma Axillare* (Lam.) Leaf Extract. *Biochemistry and Biophysics Reports*, Volume 20, p. 100699
- Maqbool, Q., Iftikhar, S., Nazar, M., Abbas, F., Saleem, A., Hussain, T., Kausar, R., Anwaar, S., Jabeen, N., 2017. Green Fabricated CuO Nanobullets via *Olea Europaea* Leaf Extract Shows Auspicious Antimicrobial Potential. *IET Nanobiotechnology*, Volume 11(4), pp. 463–468
- Muktaridha, O., Adlim, M., Suhendrayatna, I., Bakar, N.H.H.A., 2021. Photocatalytic Degradation of Skim-Latex-Vapor Odor Using Iron-Doped Zinc Oxide. *International Journal of Technology*, Volume 12(4), pp. 739–748
- Nabila, M.I., Kannabiran, K., 2018. Biosynthesis, Characterization and Antibacterial Activity of Copper Oxide Nanoparticles (CuO NPs) from Actinomycetes. *Biocatalysis and Agricultural Biotechnology*, Volume 15, pp. 56–62
- Nagar, N., Devra, V., 2018. Green Synthesis and Characterization of Copper Nanoparticles Using *Azadirachta Indica* Leaves. *Materials Chemistry and Physics*, Volume 213, pp. 44–51
- Naika, H.R., Lingaraju, K., Manjunath, K., Kumar, D., Nagaraju, G., Suresh, D., Nagabhushana, H., 2015. Green Synthesis of CuO Nanoparticles Using *Gloriosa Superba* L. Extract and Their Antibacterial Activity. *Journal of Taibah University for Science*, Volume 9(1), pp. 7–12
- Omar, M.S., Sanif, M.N.M., Omar, N.H.S., Ali, M.H.S.A.H., Taha, H., Mahadi, A.H., Soon, Y.W.,

- Ngaini, Z., Rosli, M.Y.H., Usman, A., 2020. Synthesis of Schiff Base Encapsulated ZnS Nanoparticles: Characterization and Antibacterial Screening. *International Journal of Technology*, Volume 11(7), pp. 1309–1318
- Osuntokun, J., Onwudiwe, D.C., Ebenso, E.E., 2017. Biosynthesis and Photocatalytic Properties of SnO₂ Nanoparticles Prepared Using Aqueous Extract of Cauliflower. *Journal of Cluster Science*, Volume 28(4), pp. 1883–1896
- Panigrahi, S., Kundu, S., Ghosh, S., Nath, S., Pal, T., 2004. General Method of Synthesis for Metal Nanoparticles. *Journal of Nanoparticle Research*, Volume 6(4), pp. 411–414
- Quirino, M.R., Lucena, G.L., Medeiros, J.A., Santos, I.M.G.D., Oliveira, M.J.C.D., 2018. CuO Rapid Synthesis with Different Morphologies by the Microwave Hydrothermal Method. *Materials Research*, Volume 21, p. e20180227
- Rajesh, K.M., Ajitha, B., Reddy, Y.A.K., Suneetha, Y., Reddy, P.S., 2018. Assisted Green Synthesis of Copper Nanoparticles Using *Syzygium Aromaticum* Bud Extract: Physical, Optical and Antimicrobial Properties. *Optik*, Volume 154, pp. 593–600
- Sabir, S., Arshad, M., Chaudhari, S.K., 2014. Zinc Oxide Nanoparticles for Revolutionizing Agriculture: Synthesis and Applications. *The Scientific World Journal*, Volume 2014, p. 925494
- Sankar, R., Manikandan, P., Malarvizhi, V., Fathima, T., Shivashangari, K.S., Ravikumar, V., 2014. Green Synthesis of Colloidal Copper Oxide Nanoparticles Using *Carica Papaya* and its Application in Photocatalytic Dye Degradation. *Spectrochimica Acta Part A: Molecular and Biomolecular Spectroscopy*, Volume 121, pp. 746–750
- Siddiqi, K.S., Husen, A., 2020. Current Status of Plant Metabolite-based Fabrication of Copper/Copper Oxide Nanoparticles and Their Applications: A Review. *Biomaterials Research*, Volume 24(1), pp. 1–15
- Singh, S., Kumar, N., Kumar, M., Agarwal, A., Mizaikoff, B., 2017. Electrochemical Sensing and Remediation of 4-Nitrophenol Using Bio-synthesized Copper Oxide Nanoparticles. *Chemical Engineering Journal*, Volume 313, pp. 283–292
- Sivaraj, R., Rahman, P.K., Rajiv, P., Salam, H.A., Venkatesh, R., 2014. Biogenic Copper Oxide Nanoparticles Synthesis Using *Tabernaemontana Divaricate* Leaf Extract and its Antibacterial Activity Against Urinary Tract Pathogen. *Spectrochimica Acta Part A: Molecular and Biomolecular Spectroscopy*, Volume 133, pp. 178–181
- Sohrabnezhad, S., Valipour, A., 2013. Synthesis of Cu/CuO Nanoparticles in Mesoporous Material by Solid State Reaction. *Spectrochimica Acta Part A: Molecular and Biomolecular Spectroscopy*, Volume 114, pp. 298–302
- Sone, B.T., Diallo, A., Fuku, X.G., Gurib-Fakim, A., Maaza, M., 2020. Biosynthesized CuO Nanoplatelets: Physical Properties and Enhanced Thermal Conductivity Nanofluidics. *Arabian Journal of Chemistry*, Volume 13(1), pp. 160–170
- Sundar, S., Venkatachalam, G., Kwon, S.J., 2018. Biosynthesis of Copper Oxide (CuO) Nanowires and Their Use for the Electrochemical Sensing of Dopamine. *Nanomaterials*, Volume 8(10), pp. 823–839
- Thamer, N.A., Muftin, N.Q., Al-Rubae, S.H.N., 2018. Optimization Properties and Characterization of Green Synthesis of Copper Oxide Nanoparticles Using Aqueous Extract of *Cordia Myxa* L. Leaves. *Chemistry - An Asian Journal*, Volume 30(7), pp. 1559–1563
- Yadav, S.K., Vasu, V., 2016. Synthesis and Characterization of Copper Nanoparticles, Using Combination of Two Different Sizes of Balls in Wet Ball Milling. *International Journal of Emerging Trends in Science and Technology*, Volume 3(4), pp. 2348–9480